


## ORIGINAL RESEARCH

# *Blumeria hordei* affects volatile emission of susceptible and resistant barley plants and modifies the defense response of recipient plants

Silvana Laupheimer<sup>1</sup> | Andrea Ghirardo<sup>2</sup> | Lisa Kurzweil<sup>3</sup> | Baris Weber<sup>2</sup> |  
Timo D. Stark<sup>4</sup> | Corinna Dawid<sup>3,4</sup> | Jörg-Peter Schnitzler<sup>2</sup> | Ralph Hückelhoven<sup>1</sup> 

<sup>1</sup>Chair of Phytopathology, TUM School of Life Sciences, Technical University of Munich, Freising, Germany

<sup>2</sup>Research Unit Environmental Simulation (EUS), Helmholtz Center Munich, Neuherberg, Germany

<sup>3</sup>Professorship for Functional Phytometabolomics, TUM School of Life Sciences, Technical University of Munich, Freising, Germany

<sup>4</sup>Chair of Food Chemistry and Molecular Sensory Science, TUM School of Life Sciences, Technical University of Munich, Freising, Germany

**Correspondence**

Ralph Hückelhoven,  
Email: [hueckelhoven@tum.de](mailto:hueckelhoven@tum.de)

**Funding information**

Deutsche Forschungsgemeinschaft,  
Grant/Award Number: SFB924/TP-B12;  
Deutsche Bundesstiftung Umwelt,  
Grant/Award Number: 599/20019

Edited by S.-H. Li

**Abstract**

The barley powdery mildew disease caused by the biotrophic fungus *Blumeria hordei* (*Bh*) poses enormous risks to crop production due to yield and quality losses. Plants and fungi can produce and release volatile organic compounds (VOCs) that serve as signals in plant communication and defense response to protect themselves. The present study aims to identify VOCs released by barley (*Hordeum vulgare*) during *Bh*-infection and to decipher VOC-induced disease resistance in receiver plants. VOC profiles of susceptible *MLO* wild type (*MLO* WT) and a resistant near-isogenic backcross line (*mlo5*) were characterized over time (one day or three days after *Bh* inoculation) using TD-GC/MS. Comparative analysis revealed genotype-dependent VOC profiles and significant differences in emission rates for  $\beta$ -caryophyllene, linalool, (*Z*)-3-hexenol, and methyl salicylate. Furthermore, susceptible barley plants were exposed to the complex VOC bouquet of *MLO* WT or *mlo5* sender plants in plant-to-plant communication. We found that VOC-induced resistance in receiver plants depended on the sender genotype in a *Bh* susceptibility assay. Additionally, untargeted metabolomics and gene expression studies provide evidence toward an SA-dependent pathway mediating VOC-induced resistance against powdery mildew. The exogenous application of methyl salicylate resulted in the enhanced expression of the *BARLEY CHEMICALLY INDUCED-4* marker gene and induced resistance in receiver plants. The findings suggest genotype-dependent alterations in barley VOC profiles during biotrophic plant-fungus interactions and show a VOC-mediated resistance that shares components with salicylic acid-related pathways. The VOC signals identified here could serve as non-invasive markers for disease progression in barley-powdery mildew interactions and as signals for resistance induction in recipient plants.

**1 | INTRODUCTION**

Plant volatile organic compounds (VOCs) are released into the surrounding environment as part of a regular plant metabolism. VOCs play an essential role in defense signaling and communication

between plants and are emitted in response to diverse stresses (Brilli et al., 2019; Erb, 2018; Ninkovic et al., 2021). Fungal infection-dependent modifications in VOC emissions have been shown (Ameje et al., 2018; Sulaiman et al., 2023), and the rate of VOC emission from plants and fungi varies depending on

This is an open access article under the terms of the [Creative Commons Attribution-NonCommercial](https://creativecommons.org/licenses/by-nc/4.0/) License, which permits use, distribution and reproduction in any medium, provided the original work is properly cited and is not used for commercial purposes.

© 2024 The Author(s). *Physiologia Plantarum* published by John Wiley & Sons Ltd on behalf of Scandinavian Plant Physiology Society.

physiological contexts (Morath et al., 2012; Piesik et al., 2022; Valencia-Ortiz et al., 2022).

Plants produce VOCs constitutively or induce them by stress (Dudareva et al., 2013; Loreto et al., 2014) and due to their low molecular weight and high vapor pressure, VOCs can easily diffuse through cell tissues at ambient temperatures (Mofikoya et al., 2019; Morath et al., 2012). VOCs can serve as long-distance signals in plant-to-plant communication (Baldwin & Schultz, 1983; Bitas et al., 2013) and, when triggered by pathogen attacks, herbivore damage, or wounding, can induce resistance or defense priming in neighboring plants against subsequent herbivores (Foba et al., 2023; Kim & Felton, 2013) or pathogens (Ameje et al., 2015; Brambilla et al., 2022; Hammerbacher et al., 2019; Laupheimer et al., 2023; Wenig et al., 2019). Most studies with pathogens focused on the interaction of plants with necrotrophic or hemi-biotrophic fungi (Finiti et al., 2014; Gorman et al., 2020; Kravchuk et al., 2011; Vicedo et al., 2009). As the VOC profile is based on the plant genotype, the type of damage (Mithöfer et al., 2009), and the lifestyle of the attacking pathogen (Ficke et al., 2021; Guo et al., 2021; Müller et al., 2013), we have chosen the model ascomycete *Blumeria hordei* (*Bh*) to study the effect of differential biotrophic fungal infections on VOC emissions.

*Blumeria hordei* causes the powdery mildew disease of barley and has the potential to cause drastic losses in grain quality and yield worldwide. The interaction of *Bh* and its natural host barley (*Hordeum vulgare* L.; Wyand & Brown, 2003) is well understood, and it is comparably easy to monitor fungal development on the leaf epidermis (Kita et al., 1981; Schulze-Lefert & Vogel, 2000). After the first contact of *Bh* conidia with the host tissue, differentiation of fungal structures occur within the first 24 hours: a primary germ tube develops, then the appressorial germ tube, the appressorium, and finally the haustorium consecutively appear (Aist & Bushnell, 1991; Ellingboe, 1972). Establishing the haustorium within the host epidermal cell represents the crucial step for subsequent successful fungal reproduction, as the haustorium is likely the only interface that serves pathogen nourishment. The formation of secondary hyphal structures and conidiophores on the leaf surface occurs only after successful host cell invasion (Eichmann & Hückelhoven, 2008).

Besides this interaction of *Bh* with its susceptible host, alternative host-genotype dependent interactions are also known. In particular, barley *mlo*-genotypes show recessively inherited resistance to *Bh*, which is based on the lack of a functional host MLO protein (Jørgensen, 1992; Kusch & Panstruga, 2017). The dominant MLO wild type gene (WT) hence confers susceptibility to *Bh*. The MLO gene encodes a seven-transmembrane domain protein that is thought to regulate host defense responses and calcium fluxes, but its molecular function is still incompletely understood (Büsches et al., 1997; Gao et al., 2022). The *mlo5* resistance mechanism is linked to rapid cell-wall remodeling and a cell wall papilla response that coincides with fungal failure to penetrate. Unsuccessful penetration of the attacked cell is associated with the accumulation of H<sub>2</sub>O<sub>2</sub> and phenolic compounds (Hückelhoven

et al., 1999; Röpenack et al., 1998). Apart from a genetically fixed resistance, diverse types of induced resistance are known for the interaction of barley and powdery mildew, and respective gene expression or physiological markers have been described (Beißer et al., 2000; Dey et al., 2014; Käsbauer et al., 2018; Kogel & Langen, 2005).

Regarding VOC-mediated defense mechanisms, two compounds,  $\beta$ -ionone and nonanal, were identified and have been shown to act as a signal for systemic acquired resistance (SAR) via pipelicolic acid in barley receiver plants (Brambilla et al., 2022, 2023). Also, methyl salicylate (MeSA) is known as a volatile signal associated with SAR by conversion of MeSA to salicylic acid in receiver plants (Park et al., 2007; Peng et al., 2021) and induction of plant defense responses against herbivores (Xiao et al., 2022) or pathogens (Dieryckx et al., 2015). Crop plants emit disease-specific VOCs after pathogen infection (Ficke et al., 2021), enabling the differentiation of pathogen species in the field (Thompson et al., 2021). Volatiles may serve as biocontrol agents in horticultural and agricultural integrated pest management practices or might be exploited as chemical signatures for tracking disease development in future agronomic practices or non-invasive markers in resistance breeding programs (Brilli et al., 2019).

In this study, we first investigated the VOC profile of barley during the interaction with *Bh*. We hypothesized that VOC emission is affected by infection with a biotrophic fungus over time and may differ between a susceptible (*MLO* WT) and resistant host plant genotype (*mlo5*). We then tested whether the *Bh*-induced VOC profile or specific individual VOCs can modulate the pathogen interaction outcome in VOC receiver plants. Our results show that VOC emissions are related to the genetically fixed resistance and that the corresponding VOC profiles modify the resistance level of receiver plants against a powdery mildew infection.

## 2 | MATERIALS AND METHODS

### 2.1 | Plant material and cultivation of *Blumeria hordei* (*Bh*)

Experiments were performed with  $12 \pm 1$  day-old barley plants (*Hordeum vulgare* L. cv. Ingrid) and their near-isogenic backcross line carrying the recessive *mlo5* resistance gene. Seeds were germinated for three days on wet filter paper in Petri dishes in the dark at room temperature and transferred to non-sterilized soil (CL ED73, Werke Patzer). For VOC collection and analysis, 15 individuals were grown together in a 7 x 7 cm plastic pot, representing one biological replicate. Plants were cultivated in the Fitotron SGC 120-H (Weiss Technik, Loughborough) with a 16:8 (day:night) period at  $18 \pm 2$  °C, a light intensity of  $150 \pm 2$   $\mu\text{E m}^{-2} \text{s}^{-1}$  and a relative humidity of 65%. The powdery mildew fungus *Blumeria hordei* (*Bh*) Em. Marchal race A6 served as a pathogen. It was maintained on barley cv. Golden Promise in a climate chamber MLR-351H (Sanyo, Moriguchi) at the same conditions.

## 2.2 | VOC collection and analysis

VOCs emitted by mock-treated and *Bh*-infected MLO WT and *mlo5* near-isogenic backcross line were collected using a custom-built dynamic setup. Fifteen barley individuals per pot at 11-day-old were inoculated with *Bh* spores using an inoculation tower (Laupheimer et al., 2023) with the modification of a spore density of 15–20 spores  $\text{mm}^{-2}$  and incubated for 24 or 72 hours. Additionally, VOCs were collected from system controls for background corrections. Therefore, plants were removed from the soil one day ahead of VOC collection and only VOCs from the used soil were measured. Thirty minutes before starting the VOC sampling, plants were enclosed in an oven bag (50 × 31 cm, Toppits) to acclimate. VOCs were collected for GC–MS analysis by passing air (700  $\text{mL min}^{-1}$  influx and 400  $\text{mL min}^{-1}$  outflux) for 180 minutes through glass cartridges filled with 60 mg Tenax TA 60/80 and 60 mg Carboxen 100/100 (both from Sigma-Aldrich). Qualitative VOC analysis was achieved by TD-GC–MS, as described in Ghirardo et al. (2020). Chromatograms were evaluated using the Agilent GC–MS Enhanced ChemStation, Version E.02.00.493 (Agilent). Compounds were identified by spectra matching using databases as NIST11 and Wiley (v8), and following compounds were confirmed by reference standards: (Z)-3-hexenol, (Z)-3-Hexenyl acetate, methyl salicylate, bornyl acetate, (purchased by Sigma Aldrich),  $\alpha$ -pinene,  $\beta$ -caryophyllene and linalool (purchased by Carl Roth). These reference standards were used in three independent TD-GC–MS runs for calibration at six different concentrations from 55–800  $\text{pmol l}^{-1}$  to quantify emission level of each VOC. All extracted VOC data are based on the total ion current (TIC) signal and normalized to the internal standard  $\delta$ -2-carene (859.3  $\text{pmol } \mu\text{l}^{-1}$ ) of each measurement. Data were further processed by a background correction based on four independently measured system controls, in which the VOCs emitted from the cuvette system containing pots and soil were sampled. For background correction, the mean + 2 $\sigma$  of system blanks was calculated for each compound and subtracted from each sample value. For heatmap generation, Partial least squares discriminant analysis (PLS-DA), and ANOVA data were preprocessed by  $\log_{10}$ -transformation, and pareto-scaling using MetaboAnalyst (version 5.0). For comparison of VOC chemical classes, data were corrected by their corresponding molar masses.

## 2.3 | Plant-to-plant exposure experiment

In three independently repeated plant-to-plant exposure experiments, 15 barley individuals (MLO WT or *mlo5*) per pot were used as senders. Ten barley individuals (MLO WT) served as receiver plants and were spatially separated from the senders in different cuvettes. The sender plants were inoculated in an inoculation tower as previously described in Laupheimer et al. (2023) at 24 or 72 hours before starting the experiment with a *Bh* spore density of 15–20 spore  $\text{mm}^{-2}$ . Both senders (12 or 14 days old) and receivers (12 days old) were enclosed

in oven bags and connected with a dynamic headspace system. The plant-to-plant exposure ran for 24 hours, and mock-treated plants served as control. The exposure of MLO WT plants in a custom-built setup with (Z)-3-hexenol ( $\geq 98\%$ ), linalool ( $\geq 97\%$ ), methyl salicylate ( $\geq 99\%$ ), and  $\beta$ -caryophyllene ( $\geq 98\%$ ; all purchased from Merck Millipore) was performed as previously described in Laupheimer et al. (2023).

## 2.4 | Blumeria hordei susceptibility assay

Thirteen or 15-day-old receiver plants out of the 24 h or 72 h plant-to-plant exposures were subsequently used in a susceptibility assay against *Bh*. Plants were wrapped out of the oven bag, and after 30 min acclimatization, the second leaves of five barley individuals that remained in the pot were inoculated in vivo with a *Bh* spore density of 6–10 spores  $\text{mm}^{-2}$ . Other plant individuals in the pot were removed, and tissue of the second leaves was sampled for gene expression. After five days of incubation in the Fitotron SGC 120-H (Weiss Technik, Loughborough), 2 cm long leaf segments were evaluated by macroscopically counting fungal microcolonies developing into *Bh* pustules. In total, the experimental data set represents 15 technical replicates from three independent biological experiments. One technical replicate represents one barley individual. For data of developing *Bh* pustules, one-way ANOVA with followed Tukey-test was conducted using GraphPad Prism<sup>®</sup> (version 8.01).

## 2.5 | Histological staining and microscopic analysis

The efficiency of the defense response against *Bh*-spores in the recipient plants was evaluated 30 h after inoculation. Second leaves of pre-exposed barley individuals were bleached in ethanol:acetic acid (3:1) at room temperature and sunlight. After five days, fungal structures on 5 cm leaf segments were stained with ink and quantified by counting interaction sites with bright-field microscopy. One hundred interaction sites or more per leaf were manually counted and separated to either defended appressoria or elongated secondary hyphae. The percentage of defended appressoria of the total interaction sites was calculated for five leaves as technical replicates in three independent biological experiments.

## 2.6 | Gene expression using qRT-PCR

For RNA extraction, the Direct-zol<sup>®</sup> RNA Kit (Zymo Research) was used according to the manufacturer's instructions. The amount and quality of the extracted RNA was quantified by a NanoDrop1000 (Nanodrop). cDNA was generated using Random hexamer 0.2  $\mu\text{l}^{-1}$ , 5xReaction Buffer, Thermo Scientific Ribolock RNase Inhibitor (20 U) 10 mM dNTP, and RevertAid Reverse Transcriptase (200 U). qPCR was performed using the Takyon Low ROX SYBR 2x Master Mix blue dTTP based, and the primers for *HvUBI*

(Fwd 5'AGACCATCACGCTGGAGGTG'3, rev 5'GTCGGCGTTGGGGCACTCCTT'3; AK252410), *HvPR1* (Fwd 5'AGGTGTTG-GAGCCGTAGTC'3, rev 5'AAGCTGCAAGCGTTCCGCC'3, Z26333), *HvJIP23* (Fwd 5'TGTTGCAGACTATGCCATGAA'3, rev 5'TGCCAATCGTTGACTTAGCC'3; AB251339) and *HvBCI-4* (Fwd 5'TGGGCCTATTATTCACGCT'3, rev 5'GCAGGAAAACCTTCTTCGGG'3; AJ250283). The qRT-PCR system was provided by Agilent, and data were visualized and processed using the Avira MX Software (Agilent). Data were analyzed using the delta-delta-CT-method after normalization to the mean of the *HvUBI* reference.

## 2.7 | Metabolome and lipidome procedure using UPLC-TOF-MS

Plant tissue was processed as described in Laupheimer et al. (2023). Briefly, 50 mg of frozen barley leaves were homogenized with 1 mL methanol/water 7/3 (v/v) in the Precellys® homogenizer (Bertin Technologies; 6500 rpm, 3 × 30 s, 15 s pause). The supernatant was membrane-filtered in a brown-glass vial and used for UPLC-TOF-MS analysis.

Acetonitrile, methanol (Fisher Scientific), and formic acid (≥ 99%, HiPer Solv Chromanorm®, VWR International) were of liquid chromatography/mass spectrometry (LC-MS) grade. Water used for LC-MS was purified with an AQUA-Lab-B30-Integrity system (AQUA-Lab).

Chromatographic separation was achieved on an ACQUITY UPLC® I-Class system (Waters) equipped with an ACQUITY UPLC-BEH C<sub>18</sub> column as the stationary phase (150 mm × 2.1 mm, 1.7 μm, Waters) and a mobile phase consisting of 0.1% (v/v) formic acid in water (eluent A) and 0.1% (v/v) formic acid in acetonitrile (eluent B). The flow rate was 0.4 mL min<sup>-1</sup>, and the injection volume was 3 μL. Mobile phase composition changed as follows: hold 1% B for 1 min, 6 min linear gradient from 1% B to 35% B, 1 min linear gradient from 35% B to 70% B, 1 min linear gradient from 70% B to 100% B, hold 100% B for 3 min, 0.5 min linear gradient from 100% B to 1% B, hold 1% B for 1 min. The autosampler temperature was set to 10°C, and the column temperature was 45°C.

Mass spectrometry was accomplished using the Synapt G2-S HDMS mass spectrometer (Waters) in the high-resolution mode (40 000 FWHM) and using an electrospray ionization (ESI). Scan time for the MS<sup>E</sup> method (centroid) was set to 0.1 s. The instrument was operated in positive or negative ionization mode applying the following ion source parameters: capillary voltage +2.5 kV (ESI<sup>+</sup>), -3.0 (ESI<sup>-</sup>), sampling cone 20 V, source offset 40 V, source temperature 120 °C, desolvation temperature 450°C, cone gas flow 2 L/h, nebulizer 6.5 bar and desolvation gas 850 L/h, collision energy ramp 20–40 eV. All data were lock mass corrected on the pentapeptide leucine enkephaline (Tyr-Gly-Gly-Phe-Leu, *m/z* 554.2615, [M-H]<sup>-</sup>) in a solution (1 ng l<sup>-1</sup>) of acetonitrile/0.1% formic acid 1/1 (v/v). Scan time for the lock mass was set to 0.3 s, an interval of 15 s, and three scans to average with a mass window of ±0.3 Da. Mass calibration of the Synapt G2-S in the range 50–

1200 *m/z* was performed for each measurement using a solution of sodium formate (5 mmol l<sup>-1</sup>) in 2-propanol/water 9/1 (v/v).

Metabolomic data were analyzed using the MassLynx software (version 4.1 SCN 901, Waters). Principal component analysis (PCA) for untargeted metabolomics and lipidomics was conducted using the Progenesis Q1 software (version 3.0, Waters) applying the following peak picking conditions: all runs, limits automatic, sensitivity 3, and retention time limits 0.5–11.5 min. Features used for PCA were filtered by means of ANOVA *p*-value ≤0.05 and a max. fold change of ≥2. The processed data were exported to EZinfo (version 3.0, Waters) and the matrix was analyzed by PCA with pareto-scaling. Group differences were calculated using orthogonal partial least squares discriminant analysis (OPLS-DA) and visualized in S-plots.

## 3 | RESULTS

### 3.1 | Volatile profiles of a susceptible MLO WT barley during *Bh*-infection

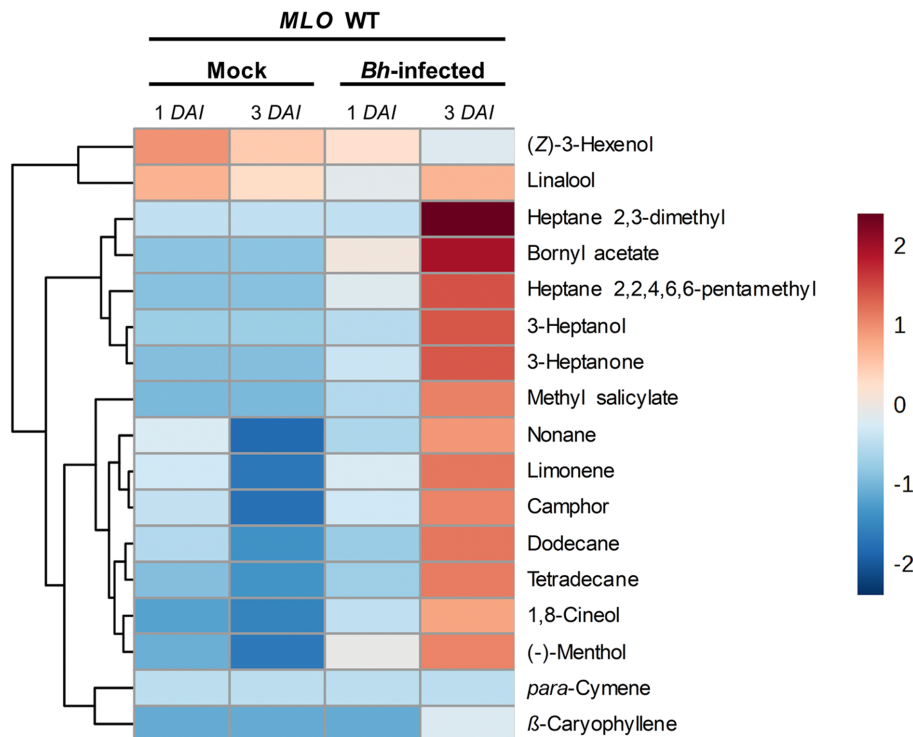
To study the effect of a *Bh*-infection on the barley volatiles, we sampled the headspace of the susceptible MLO WT strongly infected with *Bh*-spores. We compared this with VOCs of mock-treated controls at two times after infection and could identify in total 25 compounds (Table S1). An ANOVA analysis resulted in 17 compounds significantly differently (*p* < 0.05) emitted between the genotypes and the treatments (Table S3). The results are displayed as a heatmap in Figure 1 and represent VOCs in relative peak intensity.

Thirteen compounds were significantly more abundant in the headspace of *Bh*-infected susceptible barley than in the mock control, with an increasing emission from 1 to 3 DAI (Figure 1). This cluster consisted of seven compounds derived from the lipoxygenase (LOX) pathway (nonane, heptane 2,3-dimethyl, heptane 2,2,4,6,6-pentamethyl, 3-heptanol, 3-heptanone, dodecane, *n*-tetradecane), five isoprenoids (limonene, camphor, bornyl acetate, 1,8-cineole, (-)-menthol), and one benzenoid (methyl salicylate). The sesquiterpene  $\beta$ -caryophyllene metabolite was slightly more abundant in *Bh*-infected plants at day 3. By contrast, (Z)-3-hexenol, a common green leaf volatile (GLV) of the LOX pathway, was more abundant in non-infected samples and showed a reduced emission rate from 1 to 3 DAI. These data confirm that the interaction with powdery mildew alters the volatile profile of barley during infection.

### 3.2 | Comparison of VOC profiles between MLO and *mlo5* barley plants

The volatile profile of the susceptible MLO WT was compared to the volatile profile of the resistant *mlo5* backcross line. The results of hierarchical clustering of the significantly differently emitted VOCs of both genotypes were displayed in a heatmap (Figure S1, Table S1-S2) and showed a strong genotype-dependent emission pattern. We

**FIGURE 1** Volatile profiles of susceptible MLO WT barley, *Bh*-infected or mock-treated control at 1 or 3 days after inoculation (DAI). The heat map shows relative peak intensities (given as log fold change ratio and autoscaled per feature) of significantly differently emitted VOCs clustered by compounds. The scale bar ranges from red-colored cells (relatively high emission) to dark, blue-colored cells (relatively low emission). Each cell represents the average value from four independent biological replicates.



separately used a PLS-DA at 1 and 3 days after infection to classify the VOC blend based on plant resistance (*mlo5* versus susceptible MLO WT) levels. For both times, a separation between the genotypes and the treatments was observed in the PLS-DA score plot (Figure S2). For 1 DAI, the best model obtained had four components, explaining 46.5%, 14.5%, 8.4%, and 5.7% of the variation. Cross validation resulted in an accuracy of 0.82,  $R^2$  of 0.89 and  $Q^2$  of 0.71. For 3 DAI, the best PLS-DA model also had four components, explaining 42.4%, 23.8%, 9.3%, and 3.7%. In cross validation, the accuracy of this model was 0.81,  $R^2$  and  $Q^2$  were 0.95 and 0.68. To survey general discriminating factors between the susceptible MLO WT and the resistant *mlo5* the dataset was separated into chemical classes of VOCs: LOX products, monoterpenes (MT), sesquiterpenes (ST), and benzenoids (BZ). The *mlo5* genotype generally showed higher absolute peak intensities of LOX products and monoterpenes than the MLO WT with a minimum at 3 DAI after *Bh*-infection. Conversely, the MLO WT had a minimum in the mock treatment after 3 DAI (Figure 2). These results supported strongly genotype-dependent VOC profiles in both control and *Bh*-infected samples.

To search for discriminating VOCs in the whole volatile dataset (Table S1–S2), we separated the dataset into two times representing different stages of fungal development and found that  $\beta$ -caryophyllene in MLO WT and linalool in *mlo5* were significantly differently emitted (ANOVA  $p < 0.1$ ) at one day after infection (1 DAI; Figure 3A, B). *Bh*-induced emission of  $\beta$ -caryophyllene appeared in the infected MLO WT, while the *mlo5* genotype showed constitutive  $\beta$ -caryophyllene emission on a higher level than MLO WT and a decline 3 DAI with *Bh*. The emission of linalool in the *mlo5* plants strongly declined during the interaction with *Bh*, while linalool in the MLO WT showed no differences. For

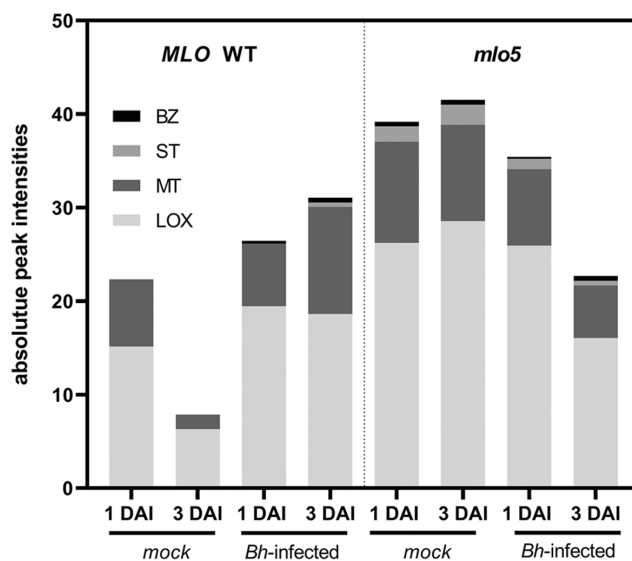


**FIGURE 2** Characterization of volatile profiles by chemical classes according to their biosynthetic origin: Lipoxigenase products (LOX), monoterpenes (MT), sesquiterpenes (ST), and benzenoids (BZ). Each bar represents the sum of all detected VOC means from four independent biological replicates. Dashed line separate between the genotypes and absolute peak intensities are given for MLO WT and *mlo5* plants; *Bh*-infected or non-infected mock control at 1 DAI or 3 DAI.

3 DAI, ANOVA supported (Z)-3-hexenol in *mlo5* and methyl salicylate (MeSA) in both genotypes to be significantly changed in abundance (Figure 3C, D). (Z)-3-hexenol was absent in the emission profile of *mlo5*

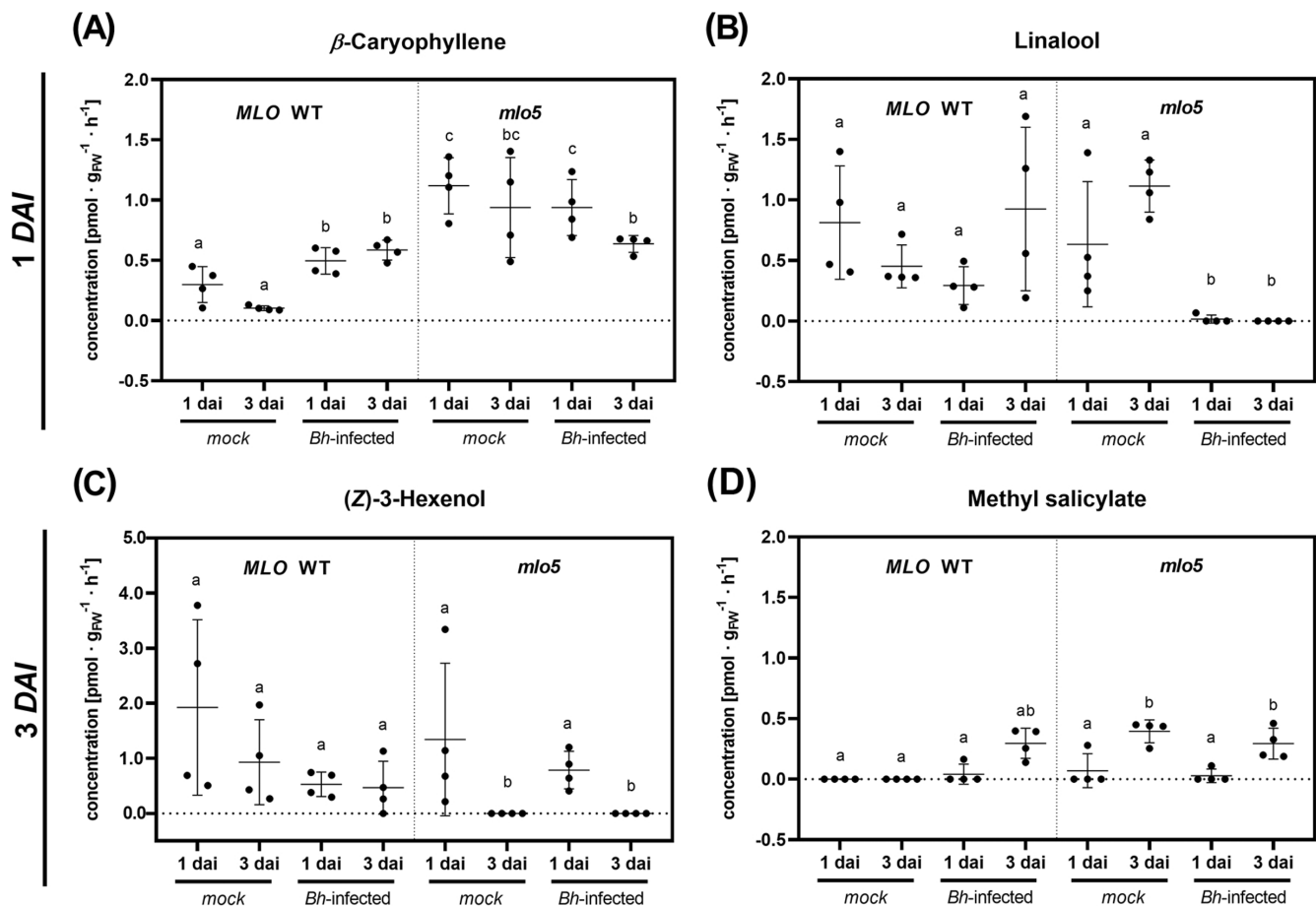


**FIGURE 3** VOC concentration of  $\beta$ -caryophyllene, linalool, (Z)-3-hexenol, and methyl salicylate. Those four compounds are significantly differently emitted (preselected by ANOVA) in the 1 DAI ( $\beta$ -caryophyllene and linalool) or 3 DAI ((Z)-3-hexenol and methyl salicylate) blend for the genotype (*MLO WT* vs. *mlo5*) and the treatment (*Bh*-infected vs. non-infected mock control). The vertical dashed line separates between the genotypes. The dot plot represents four independent biological replicates. Error bars show mean  $\pm$  SD.

plants at day 3, independent of *Bh*-treatment. In *MLO WT*, the emission of (Z)-3-hexenol tended to be lower in *Bh*-infected plants than in the mock control. Methyl salicylate was increasingly emitted during the infection with *Bh* in both genotypes. Notably, we detected a similar emission pattern of MeSA in the *mlo5* mock control.

### 3.3 | Modification of receiver plant's resistance by plant-to-plant interaction

To elucidate the effect of VOC-mediated signaling on receiver plants, we focused on the 3 DAI samples and performed an *in vivo* *Bh*-susceptibility assay. Barley plants of the susceptible cv. Ingrid WT were exposed for 24 hours to the VOC profile of 3 DAI *Bh*-infected *MLO WT* or *mlo5* and 30 minutes later inoculated with conidia of *Bh*. We found that the number of subsequently developing pustules was significantly higher in receiver plants exposed to the 3 DAI *Bh*-infected *mlo5* VOC bouquet than in those exposed to the non-infected *mlo5* mock control (Figure 4). By contrast, receiver plants exposed to the 3 DAI *Bh*-infected *MLO WT* bouquet showed

significantly fewer developing pustules than the *MLO WT* mock control. This result suggests that the induced resistance or induced susceptibility was mediated by the different genotype-dependent VOC bouquets. Next, we evaluated the fungal penetration efficiency by counting the percentage of defended appressoria in relation to the total interaction sites. For 3 DAI, the penetration efficiency was 10% lower on plants exposed to the *MLO WT* *Bh*-infected VOC profile when compared to the *MLO WT* mock. In contrast, receiver plants of the *mlo5* *Bh*-infected profile allowed for 11.5% more frequent penetration when compared to the *mlo5* mock (Figure S3). It appears that *Bh*-infected *MLO WT* volatile signals impede a successful penetration on receiver plants at an early stage of fungal development.

### 3.4 | Volatile exposure alters gene expression and induces resistance in receiver plants

To make first steps into the characterization of VOC-induced resistance, we focused on the effect of VOCs from *Bh*-infected *MLO WT* at 3 DAI. We performed a RT-qPCR on receiver plant leaves without

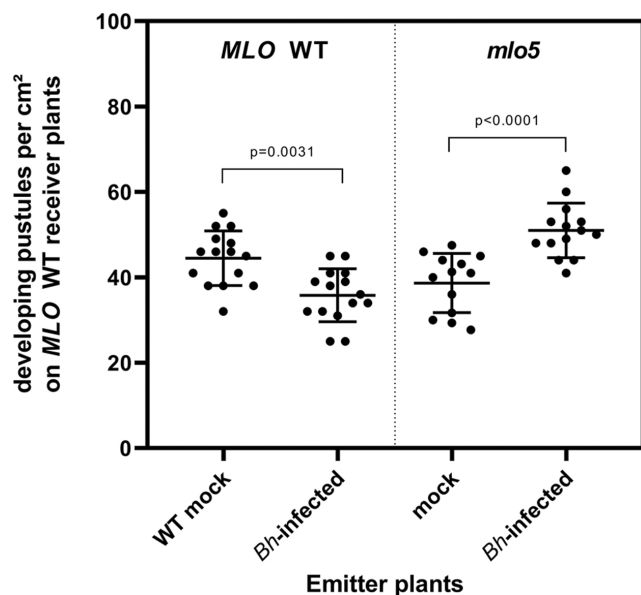


**FIGURE 4** Plant-to-plant exposure modifies barley defense response against *Bh*-infection. Quantification of developing pustules per cm<sup>2</sup> on susceptible MLO WT receiver plants after pre-exposure with the blend of *Bh*-infected MLO WT and the *mlo5* plants as emitter (3 DAI VOC profile). Error bars represent means of three independent biological replicates ± SD. The dot plot indicates the variation within the four or five technical replicates per biological replicate (one-way ANOVA, Tukey's test).

subsequent *Bh* infection to test for potential VOC-mediated marker gene expression. We used *BARLEY CHEMICALLY INDUCED-4* (*BCI-4*) as a marker gene for salicylic acid responses (Beßer et al., 2000) and *JASMONATE INDUCED PROTEIN 23* (*JIP23*) as a marker gene for jasmonic acid in barley (Kogel et al., 1995). We found a significant upregulation of the *BCI-4* gene expression in receiver plants exposed to the *Bh*-infected MLO WT bouquet compared to the mock control (Figure 5A). By contrast, the expression of *JIP23* was unchanged after VOC exposure.

As we identified the SA-derivate methyl salicylate (MeSA) in the volatile profile, we tested whether the exposure of plants to MeSA could induce a similar alteration in the gene expression of *BCI-4*. Injecting 1 µL (equivalent to 5 µM in the experimental setup) of MeSA in our dynamic headspace system resulted in an upregulated *BCI-4* gene expression (Figure 5B). No alteration was observed for *JIP23* gene expression. We also tested plants pre-exposed to individual VOCs in a *Bh*-susceptibility assay. This showed significantly reduced numbers of developing pustules in plants pre-exposed to MeSA (Figure 54A). β-Caryophyllene and linalool did not alter resistance in receiver plants, whereas (Z)-3-hexenol induced resistance (Figure 54B-D), similar to the effect previously obtained with another GLV, the (Z)-3-hexenyl acetate (Laupheimer et al., 2023). Hence, single VOCs emitted from *Bh*-infected barley plants have the potential to induce resistance to powdery mildew. However, this does not necessarily explain the resistance-modulating effects of complex VOC blends of MLO WT or *mlo5* barley plants.

### 3.5 | Volatile exposure alters metabolic profiles in receiver plants

To observe the molecular responses induced by the 3 DAI MLO WT VOC blend, we performed an untargeted metabolomics analysis of the receiver plants described above using UPLC-TOF-MS. Plants treated with the complex bouquet of *Bh*-infected MLO WT of day three were compared to those exposed to non-infected mock controls to determine differences in metabolite levels between the treatment groups using principal component analysis (PCA). Loadings and score plots are shown in Figure 55A and an ANOVA analysis ( $p < 0.05$ ) selected significant features. These features were further processed to discriminate group differences using orthogonal partial least squares discriminant analysis (OPLS-DA) and visualized in S-plots (Figure 5C). Each dot in the resulting S-plot represents a mass-to-charge-ratio-retention-time pair ( $m/z$ - $t_R$ ) which corresponds to a molecular feature. Among other unidentified features, we observed a significant upregulation of hordatine B, adenine, feruloyl quinic acid, and osmaronin in receiver plants after 24 h exposure to the headspace of *Bh*-infected barley (3 DAI).

Receiver plants exposed to MeSA were also analyzed by PCA (Figure 55B) and OPLS-DA and showed significant abundances of the lysophosphoglycerols LysoPG(18:3), LysoPG(18:2), LysoPC(18:2), and LysoPC(16:0) as well as the MeSA-derived metabolites methyl-dihydroxybenzoic acid glucosides (MeDHBAGlc) and dihydroxybenzoic acid glucoside (DHBAGlc) when compared to mock-treated controls (Figure 5D). Volatile exposure thus induced a distinct metabolome response in receiver plants, depending on the chemical signal, i.e. a single VOC or a complex VOC bouquet.

## 4 | DISCUSSION

Previously, we characterized the volatile profile of mechanically wounded barley and detected mainly green leaf volatiles that could induce resistance in receiver plants against infections with *Blumeria hordei* (*Bh*); (Laupheimer et al., 2023). Moreover, metabolome analysis indicated an upregulation of hordatines as chemical defense metabolites in receiver plants.

In this study, we characterized the volatile profile of a powdery mildew susceptible (MLO WT) and a resistant (*mlo5*) barley genotype after *Bh*- or mock-inoculation in controlled conditions comparable to Kegge et al. (2015) and Brambilla et al. (2022). We found that *Bh*-provoked VOC-mediated resistance might be related to the salicylic acid-mediated defense response. Numerous studies have demonstrated that the volatile profile of plants is affected by fungal infections (Ameje et al., 2018; Piesik et al., 2022) but predominantly focused on cell death-inducing fungi. Based on the fact that the type of damage and lifestyle of the pathogen may strongly influence the volatile signature (Ficke et al., 2021; Mithöfer et al., 2009; Nawrocka et al., 2023), we took advantage of the biotrophic interaction of *Bh* with its natural host barley. Necrotrophic fungi kill host cells, whereas biotrophic fungi depend on living cells and should, therefore, cause

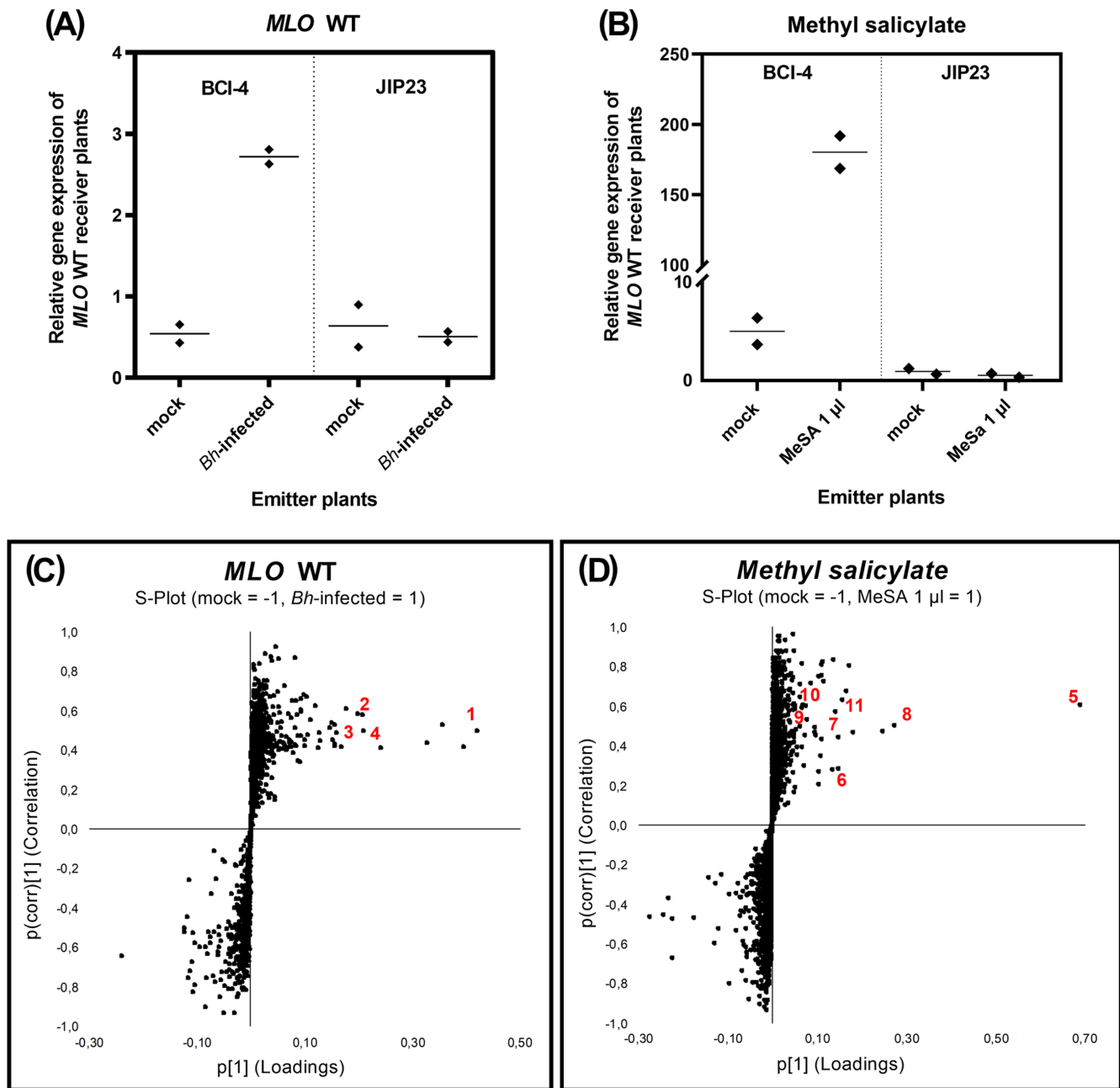


**FIGURE 5** Receiver plants show molecular responses to VOCs. qRT-PCR quantification of *BCI-4* and *JIP23* transcripts in susceptible MLO WT receiver plants after exposure with 3 DAI volatile profile of MLO WT *Bh*-infected (A) or 1  $\mu$ L of methyl salicylate (MeSA; B) compared to non-infected mock control in a dynamic headspace for 24 h. The relative gene expression of the indicated genes was calculated using the delta-delta-Ct-method and normalized to the housekeeping gene *HvUBI*. The dashed line separates between the marker genes. The dot plot indicates two independent biological replicates. One biological replicate consists of five pooled barley individual plants. S-plots of the corresponding metabolomics analysis show significant features after exposure with 3 DAI MLO WT blends (C) or MeSA (D). Features on the upper right side are upregulated in the treated receiver plants (ANOVA  $p$ -value  $\leq 0.05$ , fold change  $\geq 2$ ). 1-Hordatine B, 2-adenine, 3-feruloyl quinic acid, 4-osmaronin, 5-LysoPG(18:3), 6-LysoPG(18:2), 7-LysoPC(18:2), 8-LysoPC(16:0), 9-MeDHBAGlc (isomer 1), 10-MeDHBAGlc (isomer 2), 11-DHBAGlc. Data represent three independent biological replicates.

only little damage to the host plant within the first days after infection. We observed a change in the VOC composition and relative amounts over time during the compatible interaction of *Bh* and susceptible barley MLO WT. We assume that the VOC profiles were affected by the progressive development of fungal infections. While

1 DAI, fungal infection structure developed mainly on and inside the first attacked leaf epidermal cell, 3 DAI after inoculation, secondary hyphae developed on the leaf surface and secondary infection attempts of neighboring epidermal cells took place. A group of 13 VOCs were more strongly emitted following *Bh*-infection. We



speculate that the compatible interaction caused this VOC emission from the plant rather than the fungus because many of these compounds are typical plant VOCs and several of them were also emitted from non-infected *mlo5*-barley plants that are known to express age-dependent spontaneous defense responses (Wolter et al., 1993). Notably, as *Bh* has an obligate biotrophic lifestyle, it was not feasible to collect VOCs exclusively from the growing fungus. Mock-inoculated controls emitted a similar composition of VOCs at both 1 and 3 DAI, with the 3 DAI MLO WT control samples emitting the lowest amount (Figure 2, Table S1). The mock-inoculation might have triggered some touch-induced release of VOCs within the first day, which potentially decreased until 3 DAI due to the acclimatization time in between (Markovic et al., 2016) and the absence of continuous stress.

In MLO WT, the largest *Bh*-induced relative reduction with around 50% across all identified compounds was observed for (Z)-3-hexenol and (Z)-3-hexenyl acetate, both GLVs originating from the LOX pathway. A similar reduction of both compounds was seen in the resistant genotype (*mlo5*), again already in mock controls. Both GLVs were already identified in barley as dominant VOCs released after mechanical wounding (Laupheimer et al., 2023). On the contrary, a meta-analysis by Ameye et al. (2018), mostly based on data from cell death-inducing fungal infections, supports enhanced GLV emission during fungal infections. Sulaiman et al. (2023) reported that the obligate biotrophic fungus *Puccinia coronata* differently modifies metabolic pathways in its primary host *Avena sativa* and alternate host *Rhamnus frangula*, but in both host-pathogen-interactions LOX products were upregulated. The emission of GLVs was also positively correlated with plant growth (Escobar-Bravo et al., 2023). These data suggests that the pathogen lifestyle may influence the plant VOC composition after infection. The regulation of GLV biosynthesis and the release of certain compounds might be associated with physiological trade-offs, for instance, between growth and defense during pathogen infection.

Alkanes, dodecane and n-tetradecane, respectively, were more abundant in the headspace of *Bh*-infected MLO WT than in mock-treated MLO WT samples. Both compounds have been found as attractants in insect-plant interactions (Feng et al., 2022; Yin et al., 2022). 3-Heptanone, bornyl acetate, and MeSA were found in MLO WT samples only after *Bh*-infection, but to a certain degree also in the mock-treated resistant *mlo5* line. The function of MeSA is little described for *Triticeae* plants. Generally, MeSA is well known as a volatile signal with multiple functions in communication, plant growth, or induced resistance (Gondor et al., 2022; Gong et al., 2023). The biosynthesis of MeSA is related to salicylic acid (SA), enzymatically catalyzed by salicylic acid carboxyl methyltransferase (SAMT), and numerous studies have demonstrated the activation of defense responses by SA during interactions with biotrophic or hemi-biotrophic pathogens (Crampton et al., 2009; Hao et al., 2018). In barley, infection with *Cochliobolus sativus* activated resistance mechanisms via SA signaling rather than JA signaling (Aldaoude et al., 2022). Hückelhoven et al. (1999) observed that SA did not accumulate in the 1st leaves of young barley plants

of cv. Pallas WT and near-isogenic *mlo5*-backcross lines during *Bh*-infection. Thus, the pathogen lifestyle may affect biosynthesis and emission of MeSA.

We further analyzed the volatile blend of the *Bh*-attacked resistant *mlo5* barley, a near-isogenic backcross line of cv. Ingrid MLO WT. Barley plants belonging to MLO WT or *mlo5* showed different emissions of VOCs across the chemical classes (Figure 2) and single compounds (Figure 3, Figure S1). The *mlo5* plants constitutively produced more VOCs, especially fatty acid derivatives from the LOX pathway but also terpenoids and MeSA. Although the two barley lines are near-isogenic, the released VOCs of the mock-treated plants were qualitatively and quantitatively different. It even seems that the respective volatile profile is more affected by the genotype than the treatment. Similar results of volatile data of barley genotypes are published by Jud et al. (2018). The impact of *mlo5* introgression and backcrossing seems to affect plant responsiveness on multiple levels of gene expression (Zierold et al., 2005). Not all such changes may be causal for the resistance of *mlo5*-barley that restricts fungal penetration early without cell death of the attacked epidermal cell. However, *mlo5* mutant plants additionally exhibit early senescence, spontaneous formation of cell wall appositions and mesophyll cell death both spontaneously and after fungal infection. Mock-treated *mlo5*-barley emitted similar VOCs as *Bh*-infected MLO WT barley (Figure S1). The absence of a functional MLO gene might thus lower the threshold for hypersensitive response-like cell death in mesophyll cells (Shirasu & Schulze-Lefert, 2000; Wolter et al., 1993). It is, therefore, possible that *mlo5*-modulated differences in mock and *Bh*-infected plants partially derive from spontaneous or pathogen-induced defense reactions and secondary cell death.

We identified two compounds significantly differently emitted at 1 DAI:  $\beta$ -Caryophyllene, a sesquiterpene, and linalool, a monoterpene alcohol. Both compounds are typical plant VOCs but have been also reported as potential fungus-derived volatiles (Guo et al., 2021; Müller et al., 2013; Walther et al., 2021). Piesik et al. (2011, 2022) identified both VOCs in the blend of barley plants during interactions with *Fusarium ssp.*, but also in small amounts in the blend of mechanically injured barley. This is consistent with our observed emission levels in mock- or pathogen-inoculated samples. Both substances were found in mock-treated samples and hence cannot be of only fungal origin. Interestingly, while the mock-inoculated *mlo5* genotype showed emissions of both compounds, linalool was absent in pathogen-inoculated *mlo5* plants. This difference makes it tempting to speculate that the defense response in *mlo5* plants somehow affected the biosynthesis of linalool, although the underlying mechanism remains unknown. However, amongst others (Figures S1 and S2) linalool might be useful as a non-invasive marker for genotype-dependent *Bh*-responses in the early stages of pathogenesis.

The blends from 3 DAI, (Z)-3-hexenol and methyl salicylate (MeSA) were significantly differently emitted between the treatments and genotypes. (Z)-3-hexenol, a GLV, was not detected in the headspace of resistant *mlo5* after 3 DAI, independent of fungal inoculum. We assume that the *mlo5* genotype and associated early senescence might have caused changes in lipid metabolism and the unavailability

of precursors of (Z)-3-hexenol. Again, physiological trade-offs between plant growth and diverse metabolic defense pathways may account for VOC composition, qualitatively and quantitatively, due to the investment of anabolic building blocks and energy.

VOCs can serve as airborne signals to neighboring plants and result in alerting them about the presence of potential threats (Erb, 2018). In this study, we tested the defense responses in plants exposed to the volatile chemicals from spatially separated emitters. After exposure to the characterized VOC profiles at 3 DAI of mock or *Bh*-infected MLO WT and *mlo5* plants, we challenged VOC-pre-exposed susceptible barley with *Bh* spores and quantified the success of fungal penetration and pustule formation. Quantifying the penetration efficiency suggests a VOC-treatment effect on an early stage of fungal infection. This observation shows the role of volatiles in plant-to-plant communication and further supports the hypothesis of defense modification in barley against *Bh*-infection mediated by volatiles (Brambilla et al., 2022; Laupheimer et al., 2023). Noticeably, the observed induced resistance in receiver plants cannot be readily explained by the emission of one single compound of infected sender plants. We speculate that the VOC composition or multiple VOCs may cause synergistic effects toward induced resistance, similar to Hu et al. (2019), rather than specific compounds such as (Z)-3-hexenol or MeSA. Here, when applied purely in an exposure experiment, both compounds induce resistance in receiver plants. However, emission of (Z)-3-hexenol was reduced during *Bh*-infection in MLO WT at 3 DAI compared to the mock control and, therefore, may not be responsible for the induced resistance. On the other hand, the emission rate of MeSA was enhanced during *Bh*-infection. This might be an explanation for induced resistance in the receiver of the 3 DAI MLO WT emitter but not for the *mlo5* genotype, in which MeSA is also increased but induced resistance was subsequently not observed.  $\beta$ -Caryophyllene is known to act as an airborne signal in plant defense by modulation of jasmonic acid (JA)-mediated signaling (Frank et al., 2021), and both  $\beta$ -caryophyllene and linalool are known for their inhibitory effects on fungal growth in vivo (Quintana-Rodriguez et al., 2018). MeSA is also known for its antifungal effects (Dieryckx et al., 2015), but besides the direct antimicrobial activity, there may be an indirect protective effect of resistance induction. Application of pure  $\beta$ -caryophyllene or linalool did not cause any significant differences in the resistance of receiver plants at the concentration tested. However, it cannot be excluded that other concentrations would be biologically active. Dose-response experiments in plant-insect-interactions indicate behavioral differences of attractance or repellence using single VOCs or blends, respectively, of cereal kernels at different doses (Piesik et al., 2020; Piesik & Wenda-Piesik, 2015).

A recent study by Gondor et al. (2022) reviews the importance of MeSA as a volatile signal in plant-plant communication that induces defense mechanisms in receiver plants upon various stress conditions. MeSA is a volatile derivative of salicylic acid (SA), a small phenolic compound classified as defense-related plant hormone (An & Mou, 2011). Both compounds are known to modify antioxidant enzyme activity,

gene expression, nutrient and sugar contents in the exposed plant (Gondor et al., 2022). Also, systemic acquired resistance (SAR) is known to be activated by MeSA (Park et al., 2007; Peng et al., 2021). We found that the SA-related *BCI-4* marker gene (Beßer et al., 2000) was significantly higher expressed when plants were exposed to the complex VOC composition of 3 DAI *Bh*-infected MLO WT. A similar gene expression pattern could be induced in receiver plants exposed to pure MeSA via a dynamic headspace exposure study. We hence hypothesize that higher expression of SA-related genes might contribute to induced resistance against *Bh*-infection in receiver plants.

Untargeted metabolomics complemented our data as MeSA-related compounds were detected in plants exposed to MeSA: Dihydroxybenzoic acid glucoside (DHBAGlc) and two isomers of methyl dihydroxybenzoic acid glucoside (MeDHBAGlc) were more abundant in MeSA-exposed plants. That implies an uptake and perception of gaseous MeSA by the exposed plant resulting in MeSA metabolism. Additionally, a set of lysophospholipids accumulated in MeSA-exposed plants. Phospholipid-derived molecules are discussed as secondary messengers during pathogen attack between the plant and pathogen cells, or trigger defense-related genes (Xing et al., 2021). In *Arabidopsis thaliana*, phosphatidic acid (PA), a simple phosphoglycerolipid, has been shown to be involved in diverse abiotic stresses (Ruelland et al., 2015) and this is likely to be associated with the accumulation of PA in response to hormones like SA (Amokrane et al., 2024). Shah & Zeier (2013) reviewed airborne signals for plant communication contributing to SAR, including MeSA. An interrelationship between MeSA and non-identified lipid-based molecules or molecule complexes was demonstrated in locally affected and systemic tissues by Liu et al. (2011). Furthermore, major plant membrane lipids monogalactosyldiacylglycerol (MGDG) and digalactosyldiacylglycerol (DGDG) are required to induce SAR (Gao et al., 2014). Both lipids, MGDG and DGDG, have been found previously in barley exposed to (Z)-3-hexenyl acetate (Laupheimer et al., 2023). It appears hence possible that MeSA is converted to its active form SA as a SAR signal within plant tissues. An alternative possibility is that MeSA is connected to lipid metabolism, and lysophospholipids might have a function in SAR-like signaling in barley.

Defense-related metabolites, like hordatine B were significantly more abundant in receiver plants of the *Bh*-infected MLO WT besides adenine, feruloyl quinic acid and osmaronin. The biological functions of the latter compounds in powdery mildew resistance remain unknown in barley (Nielsen et al., 2006), but support a physiological response triggered by VOCs. Nevertheless, the accumulation of such compounds in receiver plants might indicate a metabolic response that results in the observed increased resistance toward biotrophic fungal infections. Volatile treatments may affect plant physiology at multiple layers. We observed distinct metabolite profiles in barley receiver plants of *Bh*-infected MLO WT or MeSA. This supports that MeSA alone, although it is an effective inducer of disease resistance, does not reflect and, therefore, cannot explain the resistance inducing effect of complex VOCs from *Bh*-infected barley plants.

In plants, exogenous application of MeSA results in higher resistance, e.g. of *Nicotiana benthamiana* seedlings against *Pseudomonas syringae* pv. *tabaci* (Song & Ryu, 2018) and MeSA pre-harvest treatment reduced the pathogenic effect of *Botrytis cinerea* infection on table grapes (García-Pastor et al., 2020). For barley, Brambilla et al. (2023) described that pipercolic acid concentrations increase during SAR and that pipercolic acid is involved in the emission of nonanal and  $\beta$ -ionone during infection with *Pseudomonas syringae* pv. *japonica*. We could not detect  $\beta$ -ionone nor pipercolic acid in our experiments, but instead detected nonanal, an aldehyde out of the GLVs (Tables S1 and S2). It was identified as a crucial signal in plant-to-plant defense propagation of barley before (Brambilla et al., 2022). Nonanal should be considered, among other GLVs in the volatile blend of *Bh*-infected MLO WT barley at 1 DAI, as part of the potentially causative volatile signals, although it was not significantly differently emitted in our dataset. We further found  $\alpha$ -pinene and camphene emitted from barley (Tables S1 and S2), VOCs that function in *Arabidopsis thaliana* plant-to-plant signaling during SAR (Riedlmeier et al., 2017) and might be considered as barley volatile signals in future studies.

GLVs and jasmonic acid (JA) are synthesized via the LOX pathway and positively affected by each other (Dudareva et al., 2013). Exogenous application of (Z)-3-hexenol induced resistance in receiver plants. This appears comparable to the obtained results with the related GLV (Z)-3-hexenyl acetate in an earlier study (Laupheimer et al., 2023). Therefore, we also tested the JA-related marker gene *JIP23*, but VOCs from *Bh*-infected MLO WT barley did not cause differences in *JIP23* gene expressions. Kogel et al. (1995) reported that resistance in barley against powdery mildew is not associated with a JA-related signaling pathway. Overall, our results hence rather suggest an SA-dependent pathway mediating VOC-induced resistance against powdery mildew. Future studies might provide further potential links between SA, pipercolic acid, and VOCs in barley plant-to-plant signaling.

Our study provides new insights into the modification of VOC profiles of differently resistant barley lines during infection with the biotrophic fungus *Bh*. VOCs derived from the plant-fungus interaction depend on the host genotype and corresponding type of interaction. Therefore, VOCs might be suitable for correlating volatile emissions with disease progression after infection.

#### AUTHOR CONTRIBUTIONS

S.L. and R.H. conceived the study concept and designed the experiments. S.L., C.D. and R.H. secured funding of the project. S.L. and L.K. performed the experiments and collected and processed the data. S.L. and R.H. analyzed and interpreted the data. S.L. drafted the manuscript. All authors reviewed and edited the manuscript. A.G., C.D. and R.H. supervised the project and A.G., B.W. and T.S. provided methodological support.

#### ACKNOWLEDGEMENTS

SL wants to thank Prof. Dr. Sybille Unsicker, University of Kiel, for mentoring and providing technical equipment and Dr. Hedda Schlegel-Starmann, Deutsche Bundesstiftung Umwelt (DBU), for her support.

#### FUNDING INFORMATION

This research was supported by the Deutsche Bundesstiftung Umwelt (DBU). The German Research Foundation supported the part of the Dawid lab in frame of SFB924/TP-B12.

#### DATA AVAILABILITY STATEMENT

The data supporting this study's findings are openly available in figshare at: <https://doi.org/10.6084/m9.figshare.27320754.v1>.

#### ORCID

Ralph Hückelhoven  <https://orcid.org/0000-0001-5632-5451>

#### REFERENCES

- Aist J.R., Bushnell W.R. (1991) Invasion of Plants by Powdery Mildew Fungi, and Cellular Mechanisms of Resistance. In: G. T. Cole, H. C. Hoch (Eds). *The Fungal Spore and Disease Initiation in Plants and Animals*. Springer, Boston, MA: 321–345.
- Aldaoude A., Jawhar M., Al-Shehadah E., Shoaib A., Moursel N., Arabi M.I.E. (2022) Changes in Jasmonic and Salicylic Acid Levels in Barley Challenged with *Cochliobolus sativus*. *Journal of Stress Physiology & Biochemistry*, 18: 40–46.
- Ameye M., Allmann S., Verwaeren J., Smagghe G., Haesaert G., Schuurink R.C., Audenaert K. (2018) Green leaf volatile production by plants: a meta-analysis. *The New Phytologist*, 3: 666–683.
- Ameye M., Audenaert K., Zutter N., Steppe K., van Meulebroek L., Vanhaecke L., Vleeschouwer D., Haesaert G., Smagghe G. (2015) Priming of wheat with the green leaf volatile Z-3-hexenyl acetate enhances defense against *Fusarium graminearum* but boosts deoxynivalenol production. *Plant Physiology*, 4: 1671–1684.
- Amokrane L., Pokotylo I., Acket S., Ducloy A., Troncoso-Ponce A., Cacas J.-L., Ruelland E. (2024) Phospholipid Signaling in Crop Plants: A Field to Explore. *Plants*, 11: 1532.
- An C., Mou Z. (2011) Salicylic acid and its function in plant immunity. *Journal of integrative plant biology*, 6: 412–428.
- Baldwin I.T., Schultz J.C. (1983) Rapid changes in tree leaf chemistry induced by damage: evidence for communication between plants. *Science*, 4607: 277–279.
- Beßer K., Jarosch B., Langen G., Kogel K.H. (2000) Expression analysis of genes induced in barley after chemical activation reveals distinct disease resistance pathways. *Molecular Plant Pathology*, 5: 277–286.
- Bitas V., Kim H.-S., Bennett J.W., Kang S. (2013) Sniffing on microbes: diverse roles of microbial volatile organic compounds in plant health. *Molecular Plant-Microbe Interactions*, 8: 835–843.
- Brambilla A., Lenk M., Ghirardo A., Eccleston L., Knappe C., Weber B., Lange B., Imani J., Schäffner A.R., Schnitzler J.-P., Vlot A.C. (2023) Pipercolic acid synthesis is required for systemic acquired resistance and plant-to-plant-induced immunity in barley. *Journal of Experimental Botany*, 10: 3033–3046.
- Brambilla A., Sommer A., Ghirardo A., Wenig M., Knappe C., Weber B., Amesmaier M., Lenk M., Schnitzler J.-P., Vlot A.C. (2022) Immunity-associated volatile emissions of  $\beta$ -ionone and nonanal propagate defence responses in neighbouring barley plants. *Journal of Experimental Botany*, 2: 615–630.
- Brilli F., Loreto F., Baccelli I. (2019) Exploiting Plant Volatile Organic Compounds (VOCs) in Agriculture to Improve Sustainable Defense Strategies and Productivity of Crops. *Frontiers in Plant Science*, 10: 264.
- Büschges R., Hollricher K., Panstruga R., Simons G., Wolter M., Frijters A., van Dealen R., van der Lee T., Diergaarde P., Groenedijk J., Töpsch S., Vos P., Salamini F., Schulze-Lefert P. (1997) The Barley Mlo Gene: A Novel Control Element of Plant Pathogen Resistance. *Cell*, 88: 695–705.

- Crampton B.G., Hein I., Berger D.K. (2009) Salicylic acid confers resistance to a biotrophic rust pathogen, *Puccinia substriata*, in pearl millet (*Pennisetum glaucum*). *Molecular Plant Pathology*, 2: 291–304.
- Dey S., Wenig M., Langen G., Sharma S., Kugler K.G., Knappe C., Hause B., Bichlmeier M., Babaiezed V., Imani J., Janzik I., Stempf T., Hückelhoven R., Kogel K.-H., Mayer K.F.X., Vlot A.C. (2014) Bacteria-triggered systemic immunity in barley is associated with WRKY and ETHYLENE RESPONSIVE FACTORS but not with salicylic acid. *Plant Physiology*, 4: 2133–2151.
- Dieryckx C., Gaudin V., Dupuy J.-W., Bonneau M., Girard V., Job D. (2015) Beyond plant defense: insights on the potential of salicylic and methyl-salicylic acid to contain growth of the phytopathogen *Botrytis cinerea*. *Frontiers in Plant Science*, 859.
- Dudareva N., Klempien A., Muhlemann J.K., Kaplan I. (2013) Biosynthesis, function and metabolic engineering of plant volatile organic compounds. *The New Phytologist*, 1: 16–32.
- Eichmann R., Hückelhoven R. (2008) Accommodation of powdery mildew fungi in intact plant cells. *Journal of Plant Physiology*, 1: 5–18.
- Ellingboe A.H. (1972) Genetics and Physiology of Primary Infection by *Erysiphe graminis*. *Phytopathology*, 4: 401.
- Erb M. (2018) Volatiles as inducers and suppressors of plant defense and immunity—origins, specificity, perception and signaling. *Current Opinion in Plant Biology*, 44: 117–121.
- Escobar-Bravo R., Lin P.-A., Waterman J.M., Erb M. (2023) Dynamic environmental interactions shaped by vegetative plant volatiles. *Natural product reports*, 4: 840–865.
- Feng H., Gou C., Aimaiti D., Sun P., Wang L., Hao H. (2022) Plant volatile organic compounds attractive to *Lygus pratensis*. *Open life sciences*, 1: 362–371.
- Ficke A., Asalf B., Norli H.R. (2021) Volatile Organic Compound Profiles From Wheat Diseases Are Pathogen-Specific and Can Be Exploited for Disease Classification. *Frontiers in Microbiology*, 803352.
- Finiti I., De la O Leyva, María, Vicedo B., Gómez-Pastor R., López-Cruz J., García-Agustín P., Real M.D., González-Bosch C. (2014) Hexanoic acid protects tomato plants against *Botrytis cinerea* by priming defence responses and reducing oxidative stress. *Molecular Plant Pathology*, 6: 550–562.
- Foba C.N., Shi J.-H., An Q.-Q., Le Liu, Hu X.-J., Hegab M.A.M.S., Liu H., Zhao P.-M., Wang M.-Q. (2023) Volatile-mediated tritrophic defense and priming in neighboring maize against *Ostrinia furnacalis* and *Mythimna separata*. *Pest management science*, 1: 105–113.
- Gao Q., Wang C., Xi Y., Shao Q., Li L., Luan S. (2022) A receptor-channel trio conducts Ca<sup>2+</sup> signalling for pollen tube reception. *Nature*, 607: 534–539.
- Gao Q.-M., Yu K., Xia Y., Shine M.B., Wang C., Navarre D., Kachroo A., Kachroo P. (2014) Mono- and digalactosyldiacylglycerol lipids function nonredundantly to regulate systemic acquired resistance in plants. *Cell reports*, 5: 1681–1691.
- García-Pastor M.E., Zapata P.J., Castillo S., Martínez-Romero D., Guillén F., Valero D., Serrano M. (2020) The Effects of Salicylic Acid and Its Derivatives on Increasing Pomegranate Fruit Quality and Bioactive Compounds at Harvest and During Storage. *Frontiers in Plant Science*, 11: 668.
- Ghirardo A., Lindstein F., Koch K., Buegger F., Schloter M., Albert A., Michelsen A., Winkler J.B., Schnitzler J.-P., Rinnan R. (2020) Origin of volatile organic compound emissions from subarctic tundra under global warming. *Global change biology*, 3: 1908–1925.
- Gondor O.K., Pál M., Janda T., Szalai G. (2022) The role of methyl salicylate in plant growth under stress conditions. *Journal of Plant Physiology*, 153809.
- Gong Q., Wang Y., He L., Huang F., Zhang D., Wang Y., Wei X., Han M., Deng H., Luo L., Cui F., Hong Y., Liu Y. (2023) Molecular basis of methyl-salicylate-mediated plant airborne defence. *Nature*, 622: 139–148.
- Gorman Z., Christensen S.A., Yan Y., He Y., Borrego E., Kolomiets M.V. (2020) Green leaf volatiles and jasmonic acid enhance susceptibility to anthracnose diseases caused by *Colletotrichum graminicola* in maize. *Molecular Plant Pathology*, 5: 702–715.
- Guo Y., Jud W., Weikl F., Ghirardo A., Junker R.R., Polle A., Benz J.P., Pritsch K., Schnitzler J.-P., Rosenkranz M. (2021) Volatile organic compound patterns predict fungal trophic mode and lifestyle. *Communications biology*, 1: 673.
- Hammerbacher A., Coutinho T.A., Gershenzon J. (2019) Roles of plant volatiles in defence against microbial pathogens and microbial exploitation of volatiles. *Plants*, 10: 2827–2843.
- Hao Q., Wang W., Han X., Wu J., Lyu B., Chen F., Caplan A., Li C., Wu J., Wang W., Xu Q., Fu D. (2018) Isochorismate-based salicylic acid biosynthesis confers basal resistance to *Fusarium graminearum* in barley. *Molecular Plant Pathology*, 8: 1995–2010.
- Hu L., Ye M., Erb M. (2019) Integration of two herbivore-induced plant volatiles results in synergistic effects on plant defence and resistance. *Plant, Cell & Environment*, 3: 959–971.
- Hückelhoven R., Fodor J., Preis C., Kogel K.H. (1999) Hypersensitive cell death and papilla formation in barley attacked by powdery mildew fungus are associated with hydrogen peroxide but not with salicylic acid accumulation. *Plant Physiology*, 119: 1251–1260.
- Jørgensen J.H. (1992) Discovery, characterization and exploitation of Mlo powdery mildew resistance in barley. *Euphytica*, 63: 141–152.
- Jud W., Winkler J.B., Niederbacher B., Niederbacher S., Schnitzler J.P. (2018) Volatilomics: a non-invasive technique for screening plant phenotypic traits. *Plant Methods*, 1: 1–18.
- Käsbauer C.L., Pathuri I.P., Hensel G., Kumlehn J., Hückelhoven R., Proels R.K. (2018) Barley ADH-1 modulates susceptibility to Bgh and is involved in chitin-induced systemic resistance. *Plant Physiology and Biochemistry*, 123: 281–287.
- Kegge W., Ninkovic V., Glinwood R., Welschen R.A.M., Voesenek L.A.C.J., Pierik R. (2015) Red:far-red light conditions affect the emission of volatile organic compounds from barley (*Hordeum vulgare*), leading to altered biomass allocation in neighbouring plants. *Annals of botany*, 6: 961–970.
- Kim J., Felton G.W. (2013) Priming of antiherbivore defensive responses in plants. *Insect Science*, 3: 273–285.
- Kita N., Toyoda H., Shishiyama J. (1981) Chronological analysis of cytological responses in powdery-mildewed barley leaves. *Canadian Journal of Botany*, 9: 1761–1768.
- Kogel K.H., Ortel B., Jarosch B., Atzorn R., Schiffer R., Wasternack C. (1995) Resistance in barley against the powdery mildew fungus (*Erysiphe graminis* f.sp. *hordei*) is not associated with enhanced levels of endogenous jasmonates. *European Journal of Plant Pathology*, 101: 319–332.
- Kogel K.-H., Langen G. (2005) Induced disease resistance and gene expression in cereals. *Cellular Microbiology*, 11: 1555–1564.
- Kravchuk Z., Vicedo B., Flors V., Camañes G., González-Bosch C., García-Agustín P. (2011) Priming for JA-dependent defenses using hexanoic acid is an effective mechanism to protect Arabidopsis against *B. cinerea*. *Journal of Plant Physiology*, 4: 359–366.
- Kusch S., Panstruga R. (2017) mlo-Based Resistance: An Apparently Universal "Weapon" to Defeat Powdery Mildew Disease. *Molecular Plant-Microbe Interactions*, 3: 179–189.
- Laupheimer S., Kurzweil L., Proels R., Unsicker S.B., Stark T.D., Dawid C., Hückelhoven R. (2023) Volatile-mediated signalling in barley induces metabolic reprogramming and resistance against the biotrophic fungus *Blumeria hordei*. *Plant Biology*, 1: 72–84.
- Liu P.-P., Dahl C.C. von, Park S.-W., Klessig D.F. (2011) Interconnection between methyl salicylate and lipid-based long-distance signaling during the development of systemic acquired resistance in Arabidopsis and tobacco. *Plant Physiology*, 4: 1762–1768.
- Loreto F., Dicke M., Schnitzler J.-P., Turlings T.C.J. (2014) Plant volatiles and the environment. *Plant, Cell & Environment*, 8: 1905–1908.
- Markovic D., Nikolic N., Glinwood R., Seisenbaeva G., Ninkovic V. (2016) Plant Responses to Brief Touching: A Mechanism for Early Neighbour Detection? *PLoS one*, 11: 0165742.

- Mithöfer A., Boland W., Maffei M.E. (2009) Molecular aspects of plant disease resistance. *Chemical Ecology of Plant-Insect-Interaction*, 34: 261–291.
- Mofikoya A.O., Bui T.N.T., Kivimäenpää M., Holopainen J.K., Himanen S.J., Blande J.D. (2019) Foliar behaviour of biogenic semi-volatiles: potential applications in sustainable pest management. *Arthropod-Plant Interactions*, 2: 193–212.
- Morath S.U., Hung R., Bennett J.W. (2012) Fungal volatile organic compounds: A review with emphasis on their biotechnological potential. *Fungal Biology Reviews*, 26: 73–83.
- Müller A., Faubert P., Hagen M., Castell W. Zu, Polle A., Schnitzler J.-P., Rosenkranz M. (2013) Volatile profiles of fungi--chemotyping of species and ecological functions. *Fungal genetics and biology FG & B*, 54: 25–33.
- Nawrocka J., Szymczak K., Skwarek-Fadecka M., Małolepsza U. (2023) Toward the Analysis of Volatile Organic Compounds from Tomato Plants (*Solanum lycopersicum* L.) Treated with *Trichoderma virens* or/and *Botrytis cinerea*. *Cells*, 12: 1271.
- Nielsen K.A., Hrmova M., Nielsen J.N., Forslund K., Ebert S., Olsen C.E., Fincher G.B., Møller B.L. (2006) Reconstitution of cyanogenesis in barley (*Hordeum vulgare* L.) and its implications for resistance against the barley powdery mildew fungus. *Planta*, 223: 1010–1023.
- Ninkovic V., Markovic D., Rensing M. (2021) Plant volatiles as cues and signals in plant communication. *Plant, Cell & Environment*, 4: 1030–1043.
- Park S.-W., Kaimoyo E., Kumar D., Mosher S., Klessig D.F. (2007) Methyl salicylate is a critical mobile signal for plant systemic acquired resistance. *Science*, 318: 113–116.
- Peng Y., Yang J., Li X., Zhang Y. (2021) Salicylic Acid: Biosynthesis and Signaling. *Annual Review of Plant Biology*, 72: 761–791.
- Piesik D., Bocianowski J., Sendel S., Krawczyk K., Kotwica K. (2020) Beetle Orientation Responses of *Gastrophysa viridula* and *Gastrophysa polygoni* (Coleoptera: Chrysomelidae) to a Blend of Synthetic Volatile Organic Compounds. *Environmental entomology*, 5: 1071–1076.
- Piesik D., Lemańczyk G., Bocianowski J., Buszewski B., Vidal S., Mayhew C.A. (2022) Induction of volatile organic compounds in *Triticum aestivum* (wheat) plants following infection by different Rhizoctonia pathogens is species specific. *Phytochemistry*, 113162.
- Piesik D., Pańka D., Delaney K.J., Skoczek A., Lamparski R., Weaver D.K. (2011) Cereal crop volatile organic compound induction after mechanical injury, beetle herbivory (*Oulema* spp.), or fungal infection (*Fusarium* spp.). *Journal of Plant Physiology*, 9: 878–886.
- Piesik D., Wenda-Piesik A. (2015) Sitophilus granarius responses to blends of five groups of cereal kernels and one group of plant volatiles. *Journal of Stored Products Research*, 63: 63–66.
- Quintana-Rodriguez E., Duran-Flores D., Heil M., Camacho-Coronel X. (2018) Damage-associated molecular patterns (DAMPs) as future plant vaccines that protect crops from pests. *Scientia Horticulturae*, 237: 207–220.
- Riedlmeier M., Ghirardo A., Wenig M., Knappe C., Koch K., Georgii E., Dey S., Parker J.E., Schnitzler J.-P., Vlot A.C. (2017) Monoterpenes Support Systemic Acquired Resistance within and between Plants. *The Plant Cell*, 6: 1440–1459.
- Röpenack E. von, Parr A., Schulze-Lefert P. (1998) Structural analyses and dynamics of soluble and cell wall-bound phenolics in a broad spectrum resistance to the powdery mildew fungus in barley. *The Journal of Biological Chemistry*, 15: 9013–9022.
- Ruelland E., Kravets V., Derevyanchuk M., Martinec J., Zachowski A., Pokotylo I. (2015) Role of phospholipid signalling in plant environmental responses. *Environmental and Experimental Botany*, 114: 129–143.
- Schulze-Lefert P., Vogel J. (2000) Closing the ranks to attack by powdery mildew. *Trends in Plant Science*, 8: 343–348.
- Shah J., Zeier J. (2013) Long-distance communication and signal amplification in systemic acquired resistance. *Frontiers in Plant Science*, 4: 30.
- Shirasu K., Schulze-Lefert P. (2000) Regulators of cell death in disease resistance. *Plant Molecular Biology*, 3: 371–385.
- Song G.C., Ryu C.-M. (2018) Evidence for Volatile Memory in Plants: Boosting Defence Priming through the Recurrent Application of Plant Volatiles. *Molecules and cells*, 8: 724–732.
- Sulaiman H.Y., Runno-Paurson E., Niinemets Ü. (2023) The same boat, different storm: stress volatile emissions in response to biotrophic fungal infections in primary and alternate hosts. *Plant Signaling & Behavior*, 1: 2217030.
- Thompson C.H., McCartney M.M., Roubtsova T.V., Kasuga T., Ebeler S.E., Davis C.E., Bostock R.M. (2021) Analysis of Volatile Profiles for Tracking Asymptomatic Infections of *Phytophthora ramorum* and Other Pathogens in Rhododendron. *Phytopathology*, 10: 1818–1827.
- Valencia-Ortiz M., Marzougui A., Zhang C., Bali S., Odubiyi S., Sathuvalli V., Bosque-Pérez N.A., Pumphrey M.O., Sankaran S. (2022) Biogenic VOCs Emission Profiles Associated with Plant-Pest Interaction for Phenotyping Applications. *Sensors*, 13: 4870.
- Vicedo B., Flors V., De la O Leyva, María, Finiti I., Kravchuk Z., Real M.D., García-Agustín P., González-Bosch C. (2009) Hexanoic acid-induced resistance against *Botrytis cinerea* in tomato plants. *Molecular Plant-Microbe Interactions*, 11: 1455–1465.
- Walther C., Baumann P., Luck K., Rothe B., Biedermann P.H.W., Gershenzon J., Köllner T.G., Unsicker S.B. (2021) Volatile emission and biosynthesis in endophytic fungi colonizing black poplar leaves. *Beilstein journal of organic chemistry*, 17: 1698–1711.
- Wenig M., Ghirardo A., Sales J.H., Pabst E.S., Breitenbach H.H., Antritter F., Weber B., Lange B., Lenk M., Cameron R.K., Schnitzler J.-P., Vlot A.C. (2019) Systemic acquired resistance networks amplify airborne defense cues. *Nature communications*, 1: 3813.
- Wolter M., Hollricher K., Salamini F., Schulze-Lefert P. (1993) The mlo resistance alleles to powdery mildew infection in barley trigger a developmentally controlled defence mimic phenotype. *Molecular Genetics and Genomics*, 239: 122–128.
- Wyand R.A., Brown J.K.M. (2003) Genetic and forma specialis diversity in *Blumeria graminis* of cereals and its implications for host-pathogen coevolution. *Molecular Plant Pathology*, 3: 187–198.
- Xiao D., Liu J., Liu Y., Wang Y., Zhan Y., Liu Y. (2022) Exogenous Application of a Plant Elicitor Induces Volatile Emission in Wheat and Enhances the Attraction of an Aphid Parasitoid *Aphidius gifuensis*. *Plants*, 24: 3496.
- Xing J., Zhang L., Duan Z., Lin J. (2021) Coordination of Phospholipid-Based Signaling and Membrane Trafficking in Plant Immunity. *Trends in Plant Science*, 4: 407–420.
- Yin H., Li W., Xu M., Xu D., Wan P. (2022) The role of tetradecane in the identification of host plants by the mirid bugs *Apolygus lucorum* and *Adelphocoris suturalis* and potential application in pest management. *Frontiers in physiology*, 1061817.
- Zierold U., Scholz U., Schweizer P. (2005) Transcriptome analysis of mlo-mediated resistance in the epidermis of barley. *Molecular Plant Pathology*, 2: 139–151.

## SUPPORTING INFORMATION

Additional supporting information can be found online in the Supporting Information section at the end of this article.

**How to cite this article:** Laupheimer, S., Ghirardo, A., Kurzweil, L., Weber, B., Stark, T.D., Dawid, C. et al. (2024) *Blumeria hordei* affects volatile emission of susceptible and resistant barley plants and modifies the defense response of recipient plants. *Physiologia Plantarum*, 176(6), e14646. Available from: <https://doi.org/10.1111/ppl.14646>